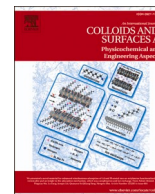




Contents lists available at ScienceDirect

Colloids and Surfaces A: Physicochemical and Engineering Aspects

journal homepage: www.elsevier.com/locate/colsurfa

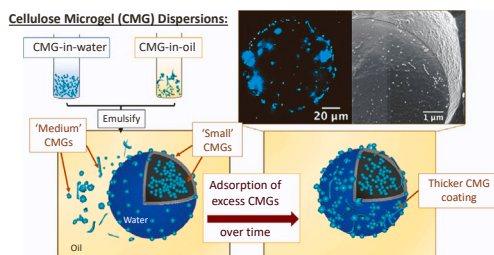
Relationship between size and cellulose content of cellulose microgels (CMGs) and their water-in-oil emulsifying capacity

Katherine S. Lefroy^a, Brent S. Murray^{a,*}, Michael E. Ries^b^a School of Food Science & Nutrition, University of Leeds, Leeds LS2 9JT, UK^b School of Physics & Astronomy, University of Leeds, Leeds LS2 9JT, UK

HIGHLIGHTS

- Cellulose microgel stabilizers provide long-term stability to W/O emulsions.
- Confocal microscopy/cryo-SEM confirmed Pickering mechanism; no cellulose network.
- Agitating during coagulation reduced microgel size (e.g. homogenization).
- Adsorption of excess microgels from oil phase increased surface coverage over time.
- Thick interfacial layers developed around water droplets, preventing coalescence.

GRAPHICAL ABSTRACT



ARTICLE INFO

Keywords:

Cellulose
Microgel
Ionic liquid
Pickering
Emulsion

ABSTRACT

Soluble polysaccharides have been used extensively as gelling/thickening agents in emulsions, but they generally display weak surface activity. Insoluble polysaccharides such as cellulose can be converted to thickening agents and even emulsifiers, but generally only after considerable chemical modification. Here we use the ionic liquid (IL) 1-butyl-3-methyl imidazolium acetate (BmimAc) to dissolve and reprecipitate cellulose in the presence of oil, i.e., a *physical* process, to tune the cellulose properties. ILs have previously been used in this way to form hydrophobic ('oily') cellulose microgels (CMGs), potentially capable of stabilizing water-in-oil (W/O) emulsions. However, these previous CMGs were made via a 'top-down' method and were relatively large and polydisperse, giving limited stability to the W/O emulsions formed. Here we demonstrate how the CMG size can be drastically reduced via a 'bottom-up' approach and employing high-pressure homogenization (HPH), thus achieving sub-micron CMG particle sizes. This has previously been impossible with other reported IL-cellulose coagulation methods and the corresponding W/O emulsions were more stable. In addition, confocal and cryo-scanning electron microscopy (SEM) revealed that the surface coverage of these CMGs on droplets increased over time, which led to the formation of even thicker interfacial layers and further enhanced emulsion stability (at least 2 months). We also demonstrate unequivocally that the stability of the W/O emulsions is indeed due to the CMGs

Abbreviations: BmimAc, 1-butyl-3-methyl imidazolium acetate; CLSM, confocal laser scanning microscopy; CMGs, cellulose microgels; cryo-SEM, cryogenic scanning electron microscopy; DLS, dynamic light scattering; FIB, focused ion beam; HIPES, high internal phase emulsions; HOSO, high oleic sunflower oil; HPH, high-pressure homogenization; IL, ionic liquid; JH, jet homogenizer; MCT, medium-chain triglyceride; O/W, oil-in-water; PSD, particle size distribution; SLS, static light scattering; WAXS, wide-angle x-ray scattering; W/O, water-in-oil.

* Corresponding author.

E-mail address: b.s.murray@leeds.ac.uk (B.S. Murray).

<https://doi.org/10.1016/j.colsurfa.2022.128926>

Received 17 February 2022; Received in revised form 31 March 2022; Accepted 1 April 2022

Available online 6 April 2022

0927-7757/© 2022 The Author(s). Published by Elsevier B.V. This is an open access article under the CC BY license (<http://creativecommons.org/licenses/by/4.0/>).

adsorbing via the Pickering mechanism, rather than forming a stabilizing cellulosic network in the continuous phase, thus providing a novel route to 'green' Pickering emulsions.

1. Introduction

Emulsions are colloidal dispersions of two immiscible liquids with different compositions, which are mixed in the presence of a stabilizer/emulsifier. Most commonly, in their simplest form, an emulsion is either made up of a water-continuous phase and an oil-discontinuous phase (oil-in-water, O/W) or vice versa (water-in-oil, W/O). Both types are used widely across many fields [1–3] and can be fabricated for different purposes, for example in the delivery of water-insoluble drugs [4], in personal care for non-greasy formulations [5] and in food for fat reduction [6,7].

Biopolymers such as polysaccharides and plant-proteins can act as emulsion stabilizers, by lowering the interfacial tension and/or changing the bulk viscosity of the system [8–11]. Depending on the biopolymer type, they can also provide electrostatic and steric stability to droplets, preventing destabilizing processes such as flocculation and coalescence. On the other hand, there are no natural biopolymers that are soluble in oil and therefore suitable as W/O emulsion stabilizers. Demand for suitable biopolymers to replace conventional synthetic surfactants has been rapidly increasing in the food, pharmaceutical and cosmetic industries, due to environmental factors [12] and toxicity issues [13], as well as a shift towards more sustainable, plant-based diets [14]. Pickering stabilizers based on materials from natural resources also offer enhanced emulsion stability [15].

Cellulose, frequently described as the most abundant natural polymer [16], is a highly attractive candidate for replacing synthetic surfactants since it is biocompatible, chemically inactive and physiologically inert [17]. Typically, cellulose displays a low contact angle with water [18,19] and is considered to preferentially stabilize water-continuous emulsions [20–24]. As a result, there are many reports of coagulated cellulose being investigated as an O/W stabilizer [20–24] and comparatively few on W/O systems. Rein et al. were able to produce W/O emulsions which displayed stability for 2 weeks, but had greater success with stabilizing O/W emulsions [25]. Pang et al. were able to produce high internal phase Pickering Emulsions (HIPes) with up to 89% water as the internal phase [15], whilst Andresen et al. produced W/O emulsions with cellulose which were remarkably stable to coalescence [19]. However in both cases, the cellulose was chemically modified, which may raise biocompatibility issues.

The discovery that ionic liquids (ILs) could be used to dissolve cellulose under mild conditions has provided a facile route for cellulose functionalization [26], with the non-toxicity and potential biodegradability of ILs making them attractive 'green' solvents [27,28]. As a result, an extensive number of reports have been published on dissolution and reprecipitation of cellulose under different conditions, to form novel cellulose stabilizers [29–32]. However, it is indeed a challenge to achieve monodisperse, regularly shaped cellulose particles using a coagulation method and sizes below 10 μm are rarely achieved. Millimeter-sized cellulose beads have been produced by employing vigorous stirring to the coagulation medium [33,34] whilst up to 1 μm -sized particles may be achieved via a sol-gel transition and reprecipitating the cellulose from an IL-in-oil emulsion [35]. In the latter case, increasing the stirring speed by just 500 rpm resulted in a decrease in the diameter of cellulose microspheres by at least half. Whilst we ourselves were able to produce cellulose microgels (CMGs) of down to 5 μm using a 'top-down' method [36], the CMG-dispersions were still relatively polydisperse and the presence of larger particles meant that consequently average droplet sizes in the W/O emulsions generally exceeded 50 μm [37]. A possible strategy for reducing the size of CMGs (and thus improving the stability of the emulsions) is to disrupt or delay the reformation of inter- and intramolecular H-bonds during coagulation,

allowing formation of smaller particles [38]. Agitation of the coagulating solution also leads to a significant difference in crystallinity of the reprecipitated cellulose [39,40], which may make it easier to disperse and may improve the cellulose surface properties.

In this work, we have fabricated highly stable W/O emulsions with CMG stabilizers of different size ranges, produced via cellulose coagulation from an IL. Different forces were employed during reprecipitation to control the CMG size and are described as dropwise ('low shear', L) and high-speed mixing ('high shear', H). High-pressure homogenization (HPH), ('very high shear', VH) was also used as a 'bottom-up' approach for producing microgels, producing a very fine dispersion of CMGs in water with particles sizes of ca. 10 nm. Particle sizing and optical microscopy were used to compare droplet sizes in the W/O emulsions stabilized by CMGs produced via the 3 methods, whilst confocal microscopy and cryo-scanning electron microscopy (SEM) provided information about surface coverage and were used to compare the morphologies of CMGs adsorbed at the interface. The mechanism of CMG stabilization was also investigated using rheological analysis, by measuring the change in bulk viscosities of emulsions over time. For each type of CMG, only physical processing methods were employed and therefore they are expected to behave in the same way as insoluble fiber during human digestion, making them suitable for food applications (as well as in other industries).

2. Materials and methods

2.1. Materials

1-Butyl-3-methyl imidazolium acetate (BmimAc) ($\geq 95\%$ purity), ethanol (absolute, 99.8%) and Calcofluor White (1 g/L) were obtained from Sigma Aldrich. 1-Butanol (Acros Organics, 99.5%) was obtained from Fisher Scientific. Cellulose powder (Vitacel L 00, full details and a wide angle x-ray scattering (WAXS) spectrum are provided in the [supporting information, table S1 and figure S1](#) respectively) and high oleic sunflower oil (HOSO, $d = 0.92 \text{ g mL}^{-1}$) were supplied by Mondelēz International. Medium-chain triglyceride oil (MCT-oil) Miglyol® 812 with a density of 0.945 g mL^{-1} at 20°C was obtained from Cremer Oleo GmbH & Co, (Germany).

2.2. CMG fabrication with low shear (L)

The first set of CMGs was fabricated by a method reported previously [36]. Briefly, cellulose powder (3 wt%) was dissolved completely in BmimAc so that a clear solution was obtained (75°C , 3–5 h). We previously determined that a concentration of 3 wt% cellulose is within the semi-dilute entangled regime and therefore sufficient for a cellulose macrogel to form [41]. HOSO or MCT-oil was then added directly to the heated solution (0.25–200 wt% oil with respect to total BmimAc volume) and mixed at high-speed with an UltraTurrax (24,000 rpm, ca. 2 min), in order to 'coat' the molecularly dissolved cellulose. Both types of oil were selected since they display similar properties to food-grade oils, for example sunflower oil, but have had most impurities removed. Less 'polar' oils were also investigated, for example tetradecane, but failed to produce CMGs with the desired stabilizing properties. For mixtures with $< 1 \text{ wt}\%$ oil, a clear solution was obtained whilst mixtures with oil contents $> 1 \text{ wt}\%$ became turbid and separated fairly rapidly (but not before they were added to the coagulation medium). Therefore, a range of oil concentrations were investigated to understand the effect of oil amount on the size and stabilizing ability of CMGs. The cellulose-BmimAc-oil mixture was then added dropwise via a syringe to anti-solvent (1-butanol, 4:1 v/v 1-butanol/oil-cellulose-BmimAc) and

stored overnight at room temperature, to produce an 'oily,' hydrophobic cellulose macrogel. Solvent exchange was then conducted as follows using the same volume of anti-solvent for each solvent change: 1-butanol; 2 x ethanol; 2 x water, with immersion in each solvent for 4–10 h. A cellulose macrogel was obtained via filtration under gravity at each stage of the solvent exchange (nylon membrane filter, 0.25 μm , 45 mm) and washed with water during the final filtration stage, to ensure complete removal of BmimAc. Oil was visible in the filtrate when a higher concentration was added (>1 wt%), indicating that the majority of the oil was not retained within the cellulose gel when an excess amount was used.

2.3. CMG fabrication via high-speed mixing (H)

The second set of CMGs was fabricated under high-speed mixing (H) during coagulation, using a high-speed blender (Ultra Turrax T 25, IKA, Germany). Cellulose was dissolved in BmimAc and mixed with oil, (as described in 2.2). The cellulose-BmimAc-oil mixtures were then added dropwise via a syringe to the anti-solvent (1-butanol, 4:1 v/v 1-butanol/oil-cellulose-BmimAc) whilst shearing (24,000 rpm, 5 min). This was so as to disrupt the structure of the cellulose as it is precipitated when coming into contact with the anti-solvent. The solution was then filtered under gravity (as described in 2.2) to collect cellulose gel particles, which were redispersed in ethanol two times (24,000 rpm, 5 min), with filtering in between, and finally redispersed in water two times (24,000 rpm, 5 min) and filtered, to complete the solvent exchange process. During the final filtration stage, the cellulose gel particles were washed with portions of water (ca. 10 mL) to ensure complete removal of BmimAc. In some cases where a very fine dispersion of microgel particles was obtained (oil content < 1 wt%), the sample was centrifuged (4,000 rpm, 15 min) to collect the CMG particles and the resulting gel pellet was washed a further 2 times with water (4,000 rpm, 15 min).

The oily cellulose hydrogels obtained in 2.2 and 2.3 (L and H) were broken down via homogenization in oil (Ultra Turrax, 24,000 rpm, 2 min) to give CMG-in-oil dispersions of varying cellulose concentrations (1–5 wv.%), where the content of cellulose is given as the weight of CMG with respect to the total oil volume. Whilst the CMGs themselves are made up of predominantly cellulose and water (and hence we refer to them as 'microgels'), they were dispersible in oil due to their hydrophobic character, imparted by the presence of oil during coagulation.

2.4. CMG fabrication using very high shear (VH)

The third method used was to coagulate cellulose from BmimAc under high pressure homogenization (HPH or 'very high' shear, VH), using a jet homogenizer (JH) as a 'microreactor' [42]. A similar approach has been reported previously for the preparation of alginate microgels, where the features of the JH are described in detail [43]. Briefly, one chamber was filled with cellulose dissolved in BmimAc (3 wt %) mixed with oil (0.25–200 wt%), total volume of mixture = 7.5 mL, prepared in the same way as in 2.2), whilst a second chamber was filled with anti-solvent (water, total volume = 15 mL). The ratios of cellulose, BmimAc, oil and water for the VH-CMGs are given in Table 1. Two pistons force the solutions out of the chambers and through a narrow hole, inducing mixing of the two solutions under highly turbulent conditions. A suspension of very fine particles (CMGs) can then be collected

Table 1

Total amounts (g) of cellulose, BmimAc, oil and water added to the JH, for fabrication of VH-CMGs. Respective densities of BmimAc, oil and water were taken as 1.05, 0.95 and 1.00 g mL⁻¹.

Sample Name	Cellulose/g	BmimAc/g	Oil/g	Water/g
VH-200	0.075	2.63	4.75	15.0
VH-1	0.22	7.80	0.07	15.0
VH-0.25	0.22	7.86	0.02	15.0

in a beaker. Pressures of 300–500 bar were used to force the two solutions through the JH. The collected CMG-in-water dispersion was then passed through the JH a further two times (at the same pressures) in order to break down any CMG aggregates and produce a finer CMG suspension (< 1 μm).

CMG-in-water dispersions (containing IL, CMGs, water and oil) were then dialyzed against pure distilled water for ca. 48 h (at room temperature), until the conductivity of the water was < 10 μS (that is to say, complete removal of the IL) [23,44]. The CMG-in-water dispersion was concentrated on a rotary evaporator (120 rpm, 55 °C) until the volume was less than half the initial volume and subsequently was dried in an oven (80 °C, 6 h), to measure the dry weight of the cellulose. The cellulose content of emulsions is given as their dry weight with respect to the oil phase: for example, for a 10:90 W/O emulsion prepared with a 1 wt% cellulose dispersion (dry weight), the cellulose content is given as 0.9 wt%.

Table 2 gives abbreviations for the samples using the following format: type of agitation-amount of oil. For example, CMGs produced via high-speed mixing with 0.25 wt% oil are denoted as "H-0.25". A schematic outlining how each type of CMG stabilizer was fabricated (L-, H- and VH-CMGs) is given in Fig. 1, for clarity.

2.5. W/O emulsions stabilized by CMGs

10 and 20 vol% water-in-oil (W/O) emulsions were formed by adding the required amount of pure water/CMG-in-water dispersion dropwise to pure oil/CMG-in-oil dispersion, under shearing (Ultra Turrax, 24,000 rpm, 2 min). For the L-/H-CMGs (produced via a 'top-down' method), pure water was added to the CMG-in-oil dispersions, whilst for the VH-CMGs (produced via a 'bottom-up' method), CMG-in-water dispersions were added to pure oil. A combination of CMG-types was also explored, where a water dispersion of VH-CMGs was added dropwise to an oil dispersion of H-CMGs. 2 mL of the emulsion was then taken and stored in a glass vial to analyze stability and sedimentation over time.

3. Characterization

3.1. Optical microscopy

CMG-in-water, CMG-in-oil dispersions and W/O emulsions were analyzed using a light microscope (Nikon, SMZ-2T, Japan), equipped with a digital camera (Leica MC120 HD) and 10x/20x lenses. A drop of each dispersion was placed on a wetted slide and covered with a coverslip (0.17 mm thickness). Images were processed using the image analysis software ImageJ.

3.2. Confocal laser scanning microscopy (CLSM)

The microstructure of W/O emulsions was analyzed via confocal laser scanning microscopy (CLSM) using a Zeiss LSM880 inverted microscope (Germany) with a 20x and 40x objective lens. Approximately 290 μL of sample was added to a wetted slide and a coverslip was placed

Table 2

Sample names for CMGs produced via various coagulation routes.

Sample Name	Method of CMG-production	Amount of Oil/wt%
L-0.25	Dropwise addition with low shear (syringe)	0.25
L-1	Dropwise addition with low shear (syringe)	1
L-200	Dropwise addition with low shear (syringe)	200
H-0.25	High-speed mixing (Ultra Turrax)	0.25
H-1	High-speed mixing (Ultra Turrax)	1
H-200	High-speed mixing (Ultra Turrax)	200
VH-0.25	Jet Homogenizer (300–500 bar)	0.25
VH-1	Jet Homogenizer (300–500 bar)	1
VH-200	Jet Homogenizer (300–500 bar)	200

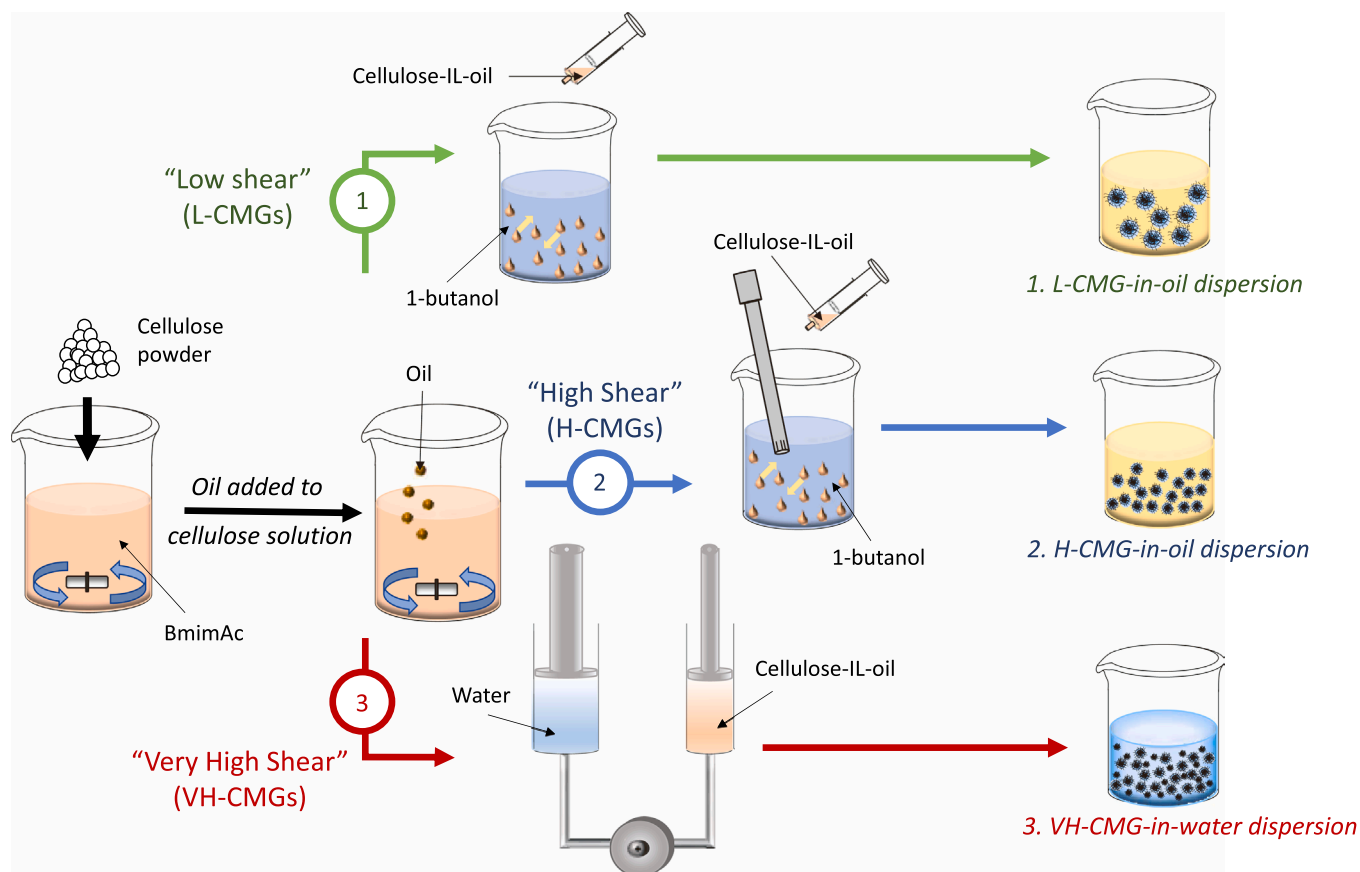


Fig. 1. Schematic to show methods for producing different CMG stabilizers: 1. ‘L-CMGs,’ produced by adding cellulose-IL-oil solution dropwise to 1-butanol; 2. ‘H-CMGs,’ produced by adding cellulose-IL-oil solution dropwise under shear to 1-butanol and 3. ‘VH-CMGs,’ produced by passing cellulose-IL-oil solution and water through a high-pressure jet homogenizer.

on top (0.17 mm thickness), ensuring that no air bubbles were trapped between the sample and coverslip. Calcofluor White was used to stain cellulose, which was added to the sample before confocal analysis (0.1 w/v %, 10% v/v stain:dispersion/emulsion). Nile Red (0.4 mg mL⁻¹ in DMSO) was added to W/O emulsions in order to stain the oil phase and analyze the shape of the water droplets (1% v/v stain:emulsion). For Calcofluor White, an excitation wavelength of 405 nm was used and emission between 415 and 470 nm measured (unless otherwise stated). For Nile Red, an excitation wavelength of 488 nm was used and emission between 420 and 520 nm measured. Images were processed using the image analysis software Zen or ImageJ.

3.3. Particle size measurements

Particle size distributions (PSDs) and ζ -potentials of CMG-in-water dispersions were measured using dynamic light scattering (DLS) via a Zetasizer Nano ZS. The dispersions were diluted before measuring: briefly, approximately two drops of sample added to a 3 mL cuvette of deionized water. Static light scattering (SLS) was performed on a Malvern Mastersizer 3000 to measure the PSD of CMG-in-oil dispersions and W/O emulsions. In all cases, the dispersions and emulsions were added dropwise to a small volume dispersion unit filled with sunflower oil and equipped with a mixer (until the laser obscuration was around 2–4%), and were therefore diluted at least 10-fold before the measurement. The refractive indices of water, MCT-oil, HOSO and cellulose were taken as 1.33, 1.45, 1.46 and 1.47 respectively and PSDs were calculated based on the Mie theory. Five measurements were taken for each sample and the average of these reported. The mean distribution of particle sizes is displayed in terms of the surface-weighted mean diameter ($d_{3,2}$), as described:

$$(d_{3,2}) = \frac{\sum_i n_i d_i^3}{\sum_i n_i d_i^2} \quad (1)$$

and the volume-weighted mean diameter ($d_{4,3}$), as described:

$$(d_{4,3}) = \frac{\sum_i n_i d_i^4}{\sum_i n_i d_i^3} \quad (2)$$

where n_i gives the number of droplets and d_i gives the diameter of the particle.

3.4. Rheological analysis

Rheological measurements were conducted using an Anton Paar MCR 302 (Anton Paar GmbH, Graz, Austria) rheometer and a 50 mm-diameter cone-plate geometry (CP50), with a fixed gap of 0.208 mm and an angle of 2 °C. Viscosity measurements were performed on freshly prepared W/O emulsions and also after 2-, 7- and 14-days storage at a fixed temperature (25 °C), within a frequency range 0.001/0.01–1000 s⁻¹. Each sample was heated to the required temperature and allowed to equilibrate for 3 min before the measurements were performed. A Peltier hood system was used for additional temperature control. All raw data was analyzed using the RheoCompass software.

3.5. Cryogenic scanning electron microscopy (cryo-SEM)

CMG-in-oil dispersions and W/O emulsions were filled in two freezing rivets and rapidly frozen in slushed nitrogen. Frozen samples were then transferred under vacuum via a cryo shuttle into a Quorum PP3010 cryo preparation chamber, which was kept under high vacuum

and at $-140\text{ }^{\circ}\text{C}$. Each sample was fractured with a cooled knife and then sublimed for approximately 3 min at $-90\text{ }^{\circ}\text{C}$, and sputter-coated with a thin layer of Iridium. Finally, they were transferred to a Thermo scientific Helios G4 CX DualBeam (focused ion beam scanning electron microscope; FIB-SEM), operating at 2 kV and 0.1 nA. The FIB-SEM was fitted with a cold stage ($-140\text{ }^{\circ}\text{C}$) and cold finger ($-175\text{ }^{\circ}\text{C}$) to reduce ice contamination and a Through the Lens (TLD) detector was used.

4. Results and discussion

4.1. L- and H-in-oil dispersions

Firstly, CMGs fabricated with low shear (L) were analyzed, which involved breaking the cellulose macrogels down into CMG-in-oil dispersions ('top-down' method). Optical micrographs and PSDs of L-in-oil dispersions at various concentrations are given in supporting information (Fig. S2). As the concentration of CMG ([CMG]) in the dispersion increases, the average size generally increased: $d_{3,2}$ values of 9.73 ± 0.99 , 10.2 ± 1.1 and $52.4 \pm 1.9\text{ }\mu\text{m}$ were obtained for 2, 4 and 6 wv.% L-in-oil dispersions, respectively. Furthermore, CMG-flocculation was visible using optical microscopy when [CMG] exceeded 5 wv.% (Fig. S2c), which was reflected by a sharp increase in $d_{4,3}$ (29.7 ± 4.4 and $71.7 \pm 3.0\text{ }\mu\text{m}$ for 4 and 6 wv.% [CMG] respectively). However, the particles were weakly aggregated since they could be broken up by dilution and therefore could be redispersed upon emulsification via homogenization. It was also observed that the sizes of L-CMGs appeared

quite different in the confocal and optical micrographs (Fig. 2b and 2). Whilst flocculation is less visible in the former case, it is likely that the Calcofluor White signal from the larger CMGs dominates and therefore smaller CMGs are less visible in the confocal image, compared to the optical image. This will be expanded on later in Section 4.7.

High-speed mixing (H) during coagulation was also adopted to try to reduce the CMG particle size and therefore the W/O droplet size that they stabilize. Fig. 2a shows the PSDs of L- and H-in-oil CMG dispersions, to provide a comparison between the two coagulation routes. Clearly the introduction of agitation during coagulation had an effect on the CMG particle sizes, with the average size being approximately 10 times smaller for the H-CMGs compared to the L-CMGs at the equivalent concentrations. This was confirmed by CLSM (Fig. 2b), where it appeared that smaller and more homogeneous particles could be produced by introducing high shear. It should be noted that the staining agent appear to be inhomogeneously distributed in the micrograph (Fig. 2b), which we attribute to the inhomogeneous structure of the cellulose macrogels (figure S2d) and therefore the CMGs. In both cases, the amount of oil added during coagulation appeared to have no effect on the particle sizes of the L- and H-CMGs (data not shown) and therefore we directly compare CMGs with various quantities of oil.

4.2. Particle size of W/O emulsions stabilized by L- and H-CMGs

Various concentrations of L- and H-in-oil CMG dispersions ([CMG] = 1–5 wv.% of oil volume) were used to fabricate W/O emulsions, to assess

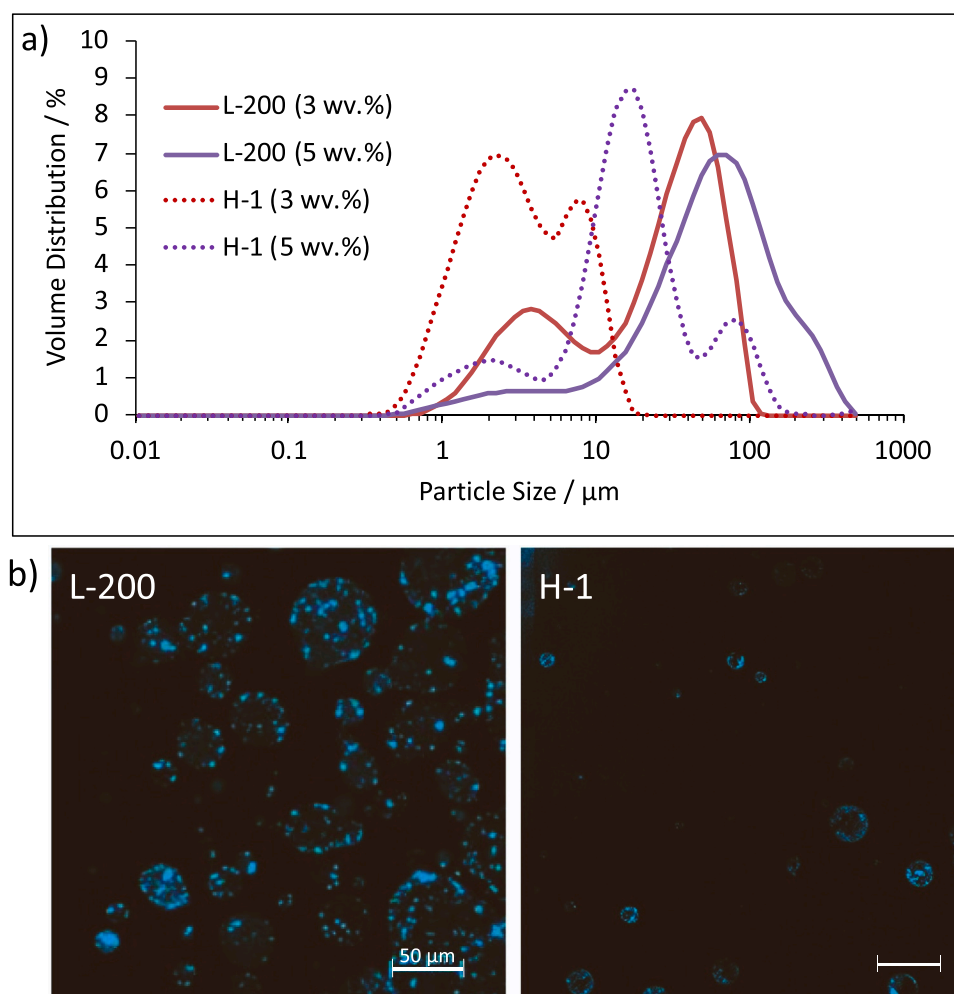


Fig. 2. a) PSDs of CMG-in-oil dispersions (3 wv.% = red and 5 wv.% = purple; L = solid lines and H = dashed lines) from L-200 and H-1; b) confocal micrographs of CMG-in-oil dispersions (3 wv.%). Scale bar = 50 μm , shown at the bottom right in white.

the effect of [CMG] on emulsion stability. An oil-continuous emulsion was produced for all concentrations of CMG, as determined by the drop test method.

Fig. 3a and b give the optical micrographs and PSDs respectively of W/O emulsions with various L-200 concentrations. From the micrographs, it appears that the droplet size of the emulsions decreases slightly and becomes more uniform as the concentration of L-200 increases, with the 4 and 5 wv.% CMG-stabilized emulsions giving the most homogeneous appearance. However, the droplet size does not appear to change significantly between [CMG] = 2–5 wv.% according to the PSDs, suggesting that a ‘threshold’ concentration is reached at 2 wv.% CMG and additional CMGs at higher concentrations do not affect droplet size but may increase surface coverage. In addition, some very small particles are visible in the optical micrographs and a corresponding peak appears in the PSD at ca. 1 μm , indicating the presence of

small CMGs which do not initially adsorb to the water-oil interface. This will be discussed further in Section 4.7. The average size from the PSDs does not appear to correlate with the size of droplets visible under the microscope, probably due to the presence of flocculated structures that were not broken down in the Mastersizer measurements due to insufficient stirring speeds (<2000 rpm). The size distribution for the 1 wv.% emulsion was significantly broader, in agreement with the larger, non-spherical droplets visible in the micrograph (Fig. 3a, shown by red arrows). This indicates some droplet coalescence is occurring and a minimum [CMG] of 2 wv.% is required for stability.

The degree of interfacial coverage of water droplets by CMGs was demonstrated via CLSM (Fig. 4). At low [CMG] (1 wv.%), there appeared insufficient CMG covering the droplet interface, hence explaining why destabilization processes such as coalescence and flocculation would be expected to occur [45]. This was confirmed by a rapid increase in

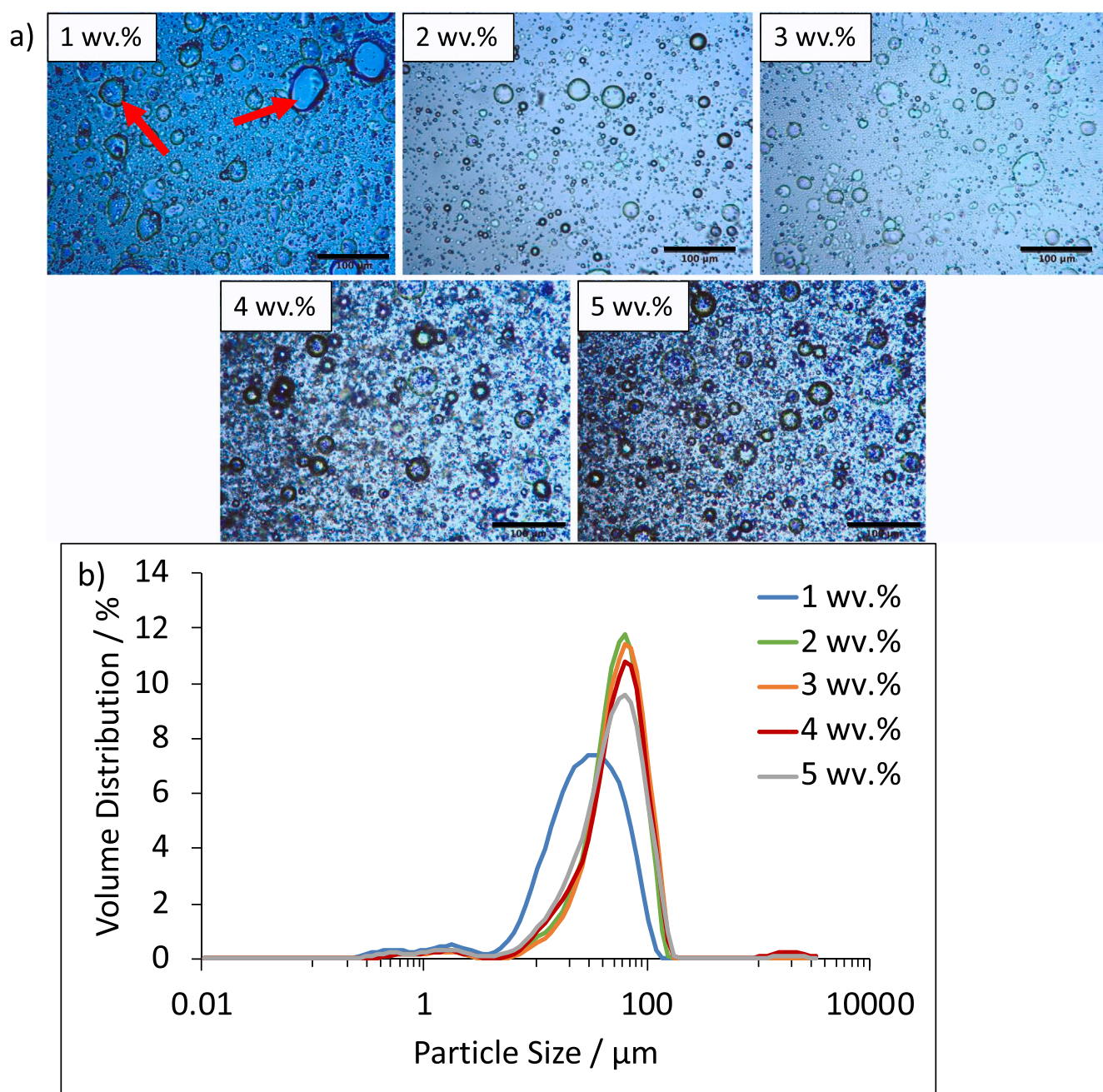


Fig. 3. a) Optical micrographs (scale bar = 100 μm , shown at the bottom right in black). The red arrows indicate coalescence; b) PSDs of 20:80 W/O emulsions stabilized by L-200 (1 wv.% = blue; 2 wv.% = green; 3 wv.% = orange; 4 wv.% = red and 5 wv.% = grey).

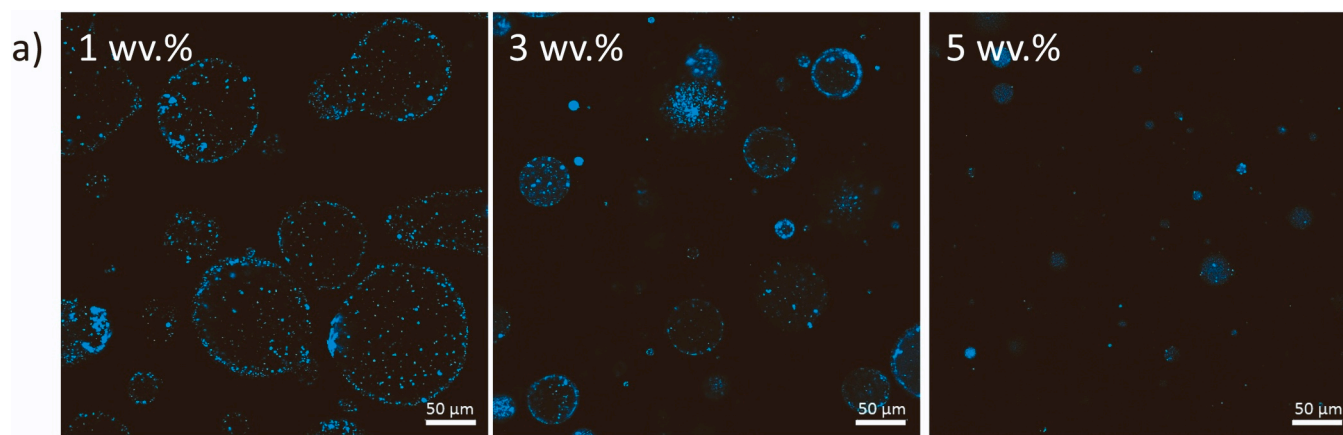


Fig. 4. Confocal micrographs of 20:80 emulsions stabilized by L-200 (1, 3 and 5 wt.%, from left to right). Scale bar = 50 μm , shown at the bottom right in white.

sediment height upon formation of the emulsion, plus after 2 weeks storage, the emulsion layer was almost completely clear (Fig. S3). At $[\text{CMG}] > 1$ wt.%, a stable emulsion could be formed with sufficient CMG droplet coverage to delay coalescence, again indicating a ‘threshold’ concentration of 2 wt.%. Furthermore, the emulsion layer was still turbid after 3 weeks, however it is unclear from the confocal micrographs in Fig. 4 whether interfacial coverage increased in the ‘fresh’ emulsions from 3 to 5 wt.% CMG. Thus it cannot be confirmed if ‘excess’ CMGs are initially located in the continuous phase or adsorbing at the interface to form multilayers.

W/O emulsions stabilized by H-CMGs were fabricated in the same way as the L-CMGs, to compare the effect of CMG particle size on emulsion stabilizing ability. Confocal images for emulsions stabilized by H-1 and L-200 are given in Fig. 5a and b, comparing the appearance of the emulsions. Although once again the PSDs were not significantly different between the H-1 and L-200-stabilized emulsions (data not shown), the droplet sizes appeared much smaller in the confocal micrographs for the former. Furthermore, the $d_{3,2}$ value of the H-CMG emulsions remained stable over time and smaller droplets were visible after 1 week storage, whilst the average droplet size for L-CMG

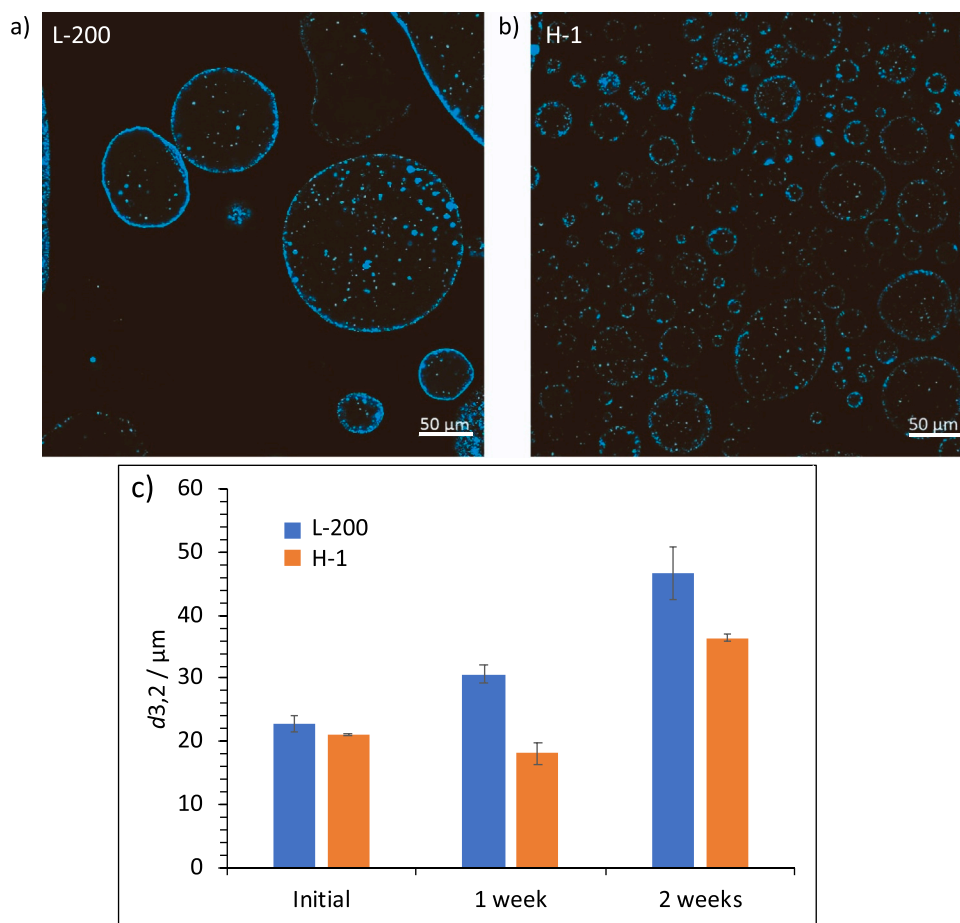


Fig. 5. Confocal images of 20:80 emulsions stabilized by a) L-200 and b) H-1. Scale bar = 50 μm , shown at the bottom right in white; c) average droplet sizes ($d_{3,2}$) over time of 20:80 emulsions stabilized by L-200 (blue) and H-1 (orange). Error bars give the uncertainties in the measurements.

emulsions appeared to steadily increase and reached almost double the initial $d_{3,2}$ value after 2 weeks (Fig. 5c). Therefore, introducing high-speed mixing during cellulose coagulation not only reduced the CMG size but also improved the emulsion system in terms of smaller and more stable water droplets. The ability to form smaller droplets minimized gravity creaming/sedimentation effects and therefore improved emulsion stability [46].

Droplet sizes and surface coverage of W/O emulsions stabilized by H-CMGs above the ‘threshold’ concentration (3 and 5 wv.%) were also compared (Fig. S4). Again, the PSDs were almost identical and little difference in coverage could be observed using CLSM.

4.3. VH-in-water dispersions

Finally, a third route for cellulose coagulation was investigated using HPH, in an attempt to reduce the particle size even further by ensuring mixing of the cellulose-BmimAc-oil mixture and the anti-solvent under highly turbulent shear conditions. In contrast to the previous methods, water alone was used as anti-solvent for this coagulation route (rather than 1-butanol followed by a solvent exchange, as described for L-CMGs and H-CMGs in 2.2 and 2.3). This was because particles produced under HPH were too fine to be collected via filtration and therefore the use of HPH describes a ‘bottom-up’ approach to microgelation, as opposed to fabrication of a larger macrogel and subsequent break-down (‘top-down’). To form W/O emulsions from the VH-CMGs, CMG-in-water dispersions were added dropwise to pure oil, therefore limiting the maximum CMG concentration according to the amount of water in the emulsion (20 vol%).

Fig. 6a and b give the appearance and PSDs respectively of various VH-in-water dispersions. (Some samples of VH-in-water dispersions were dried to determine the amount (wt%) of cellulose + oil, as outlined in 2.4). Generally, VH-CMGs were at least an order of magnitude smaller in size than the L- and H-CMGs, and the PSDs were much narrower. This was expected because the JH results in very high fluid velocities and highly turbulent conditions, inducing cavitation and restricting the

growth of nascent microgel particles and thus producing much more fine and monodisperse dispersions [43]. However, when the dispersions were concentrated the CMGs began to aggregate, and in those containing the highest [CMG] 2 peaks were observed in the PSD (Fig. 6b, [CMG] = 1.217 wt%). Furthermore, aggregation of particles was confirmed via optical microscopy at much lower concentrations for CMG-in-water compared to the CMG-in-oil dispersions (L- and H-CMGs described in 4.1), plus large length-scale cellulose networks became visible. Despite this, aggregates appeared to be made up of homogeneous CMG particles with regular morphologies and were loosely bound, and therefore easily broken up by re-dilution of the CMG-in-water dispersions.

4.4. Particle size of W/O emulsions stabilized by VH-CMGs

Various concentrations of VH-in-water dispersions were used to explore whether cellulose aggregation influences the W/O stabilizing ability of the CMGs. Fig. S5a and b give the optical micrographs and PSDs of ‘fresh’ W/O emulsions with 0.278 and 0.836 wt% VH-1 respectively. A slightly narrower PSD was measured for the emulsion with the higher [CMG] (0.836 wt%), but no significant difference in the appearance of the emulsions was observed. Droplet sizes were initially reduced compared to W/O emulsions stabilized by L- and H-CMGs, which is probably due to the higher emulsion efficiency of the smaller, more homogeneous VH-CMGs and their faster diffusion to the interface [47–49]. However, since smaller particles generally require greater number surface coverage for stabilization of droplets compared to larger, more irregularly-shaped particles [50], the concentrations of VH-CMGs in the W/O emulsions were insufficient to prevent destabilization processes over time. PSDs of the emulsions were measured 3 h later (data not shown) and in both cases, bimodal PSDs were obtained for both 0.278 and 0.836 wt%-stabilized emulsions with a comparatively large second peak. The $d_{4,3}$ values increased dramatically over 3 h (75.1 ± 9.2 – $251 \pm 19.5 \mu\text{m}$ and 25.2 ± 1.2 – $336 \pm 36.5 \mu\text{m}$ for 0.278 and 0.836 wt%-emulsions, respectively), indicating the presence of larger structures in the emulsions. Upon storage for 1 week, large

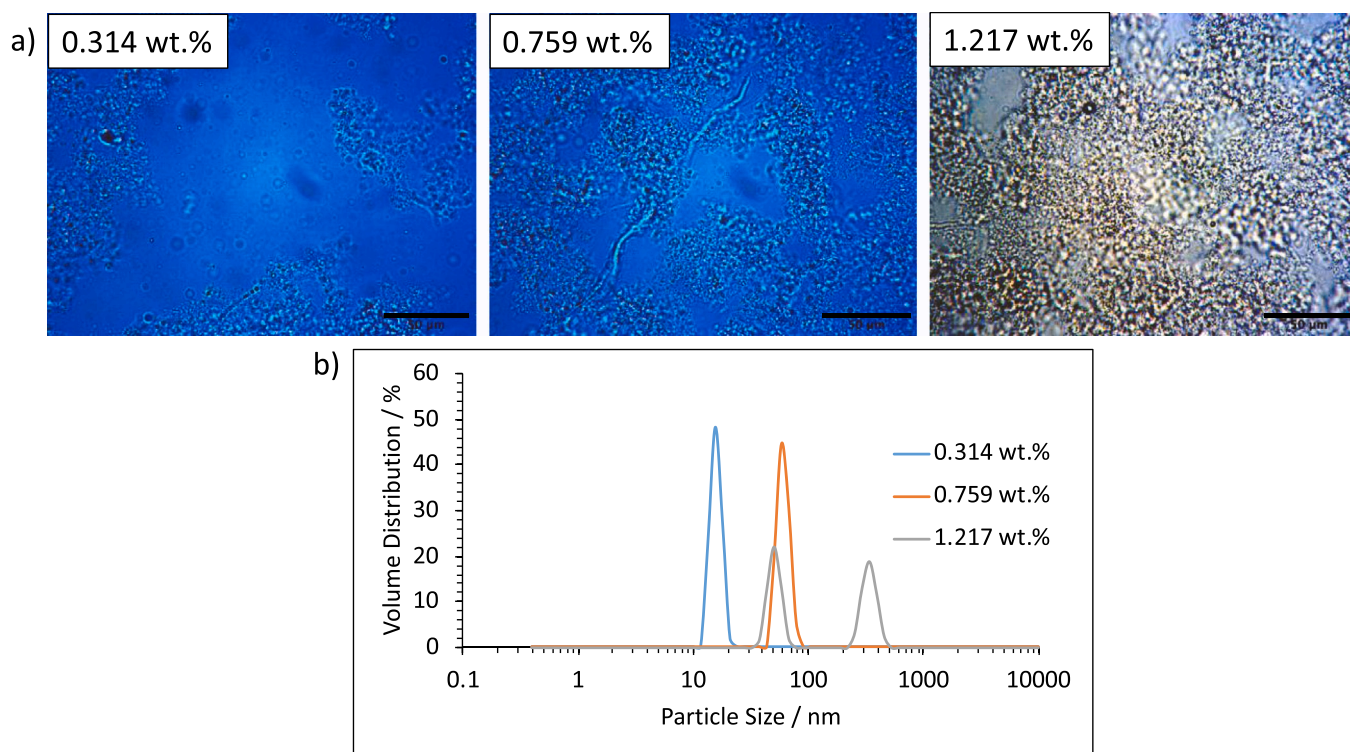


Fig. 6. a) Optical micrographs and b) PSDs of VH-0.25-in-water dispersions at various concentrations (0.314 wt% = blue; 0.759 wt% = orange and 1.217 wt% = grey). Scale bar = 50 μm, shown at bottom right in black.

droplets were visible under the microscope (figures S5c and d) and the PSD shifted significantly to larger sizes, indicating further increase in droplet sizes and/or possible further aggregation. The bottom water layer of the emulsions was turbid after 1 week (not shown), indicating that particularly large cellulose aggregates had sedimented out, therefore probably leaving a very low concentration of CMG in the emulsion layer.

Thus, although the smallest and narrowest PSDs were achieved for the VH-CMGs using a 'bottom-up' approach, the use of the JH meant that a very fine gel particle water dispersion was obtained and therefore the stabilizer had to be introduced in the discontinuous phase (water), as opposed to the continuous phase (oil). It did not seem possible or desirable to increase this concentration further (via evaporation or centrifugation), because this just led to increased viscosity of the aqueous phase and CMG aggregates. Consequently, a lower [CMG] as stabilizer was introduced in the system compared to the two previous, 'top-down' methods and although the VH-CMGs were smaller, apparently the interfacial coverage was not high enough to prevent some W/O emulsion destabilization [1].

4.5. O/W emulsions stabilized by VH-CMGs

It was considered that the properties of the VH-CMGs are expected to be different to the L-/H-CMGs, due to both the type of coagulant and the method of coagulation.

Firstly, only water was used for the VH-CMGs (2.4), whilst 1-butanol (followed by ethanol and water) were used for the L- and H-CMGs (2.2 and 2.3). Changing the anti-solvent is known to affect the properties of the reprecipitated cellulose material [51–53]: since water has a much higher affinity for both cellulose and BmimAc (compared to 1-butanol), it mixes evenly throughout the solution and supplies intermediate

hydrogen bonds during coagulation, leading to more crystalline cellulose [54]. On the other hand, 1-butanol is expected to diffuse into the coagulating solution at a slower rate and a more amorphous material is obtained [52]. Secondly, cellulose was coagulated under highly turbulent conditions for the VH-CMGs via a 'bottom-up' approach. This is expected to further facilitate rapid mixing of the anti-solvent and IL solution (which is already assisted by the use of a faster diffusing anti-solvent), and results in a 'hard' coagulation [52]. Therefore, less oil may be entrapped within the gel structure, making the VH-CMGs less suitable as W/O stabilizers and less 'hydrophobic' compared to the L-/H-CMGs, which are obtained via a 'softer' coagulation route.

To understand more about the surface properties of VH-CMGs, attempts were made to fabricate O/W emulsions with VH-1. This was to compare their suitability as oil-continuous versus water-continuous stabilizers. Optical micrographs of the emulsions on day 1 along with average droplet size ($d_{4,3}$) values, over a period of 2 weeks, are given in the supporting information (Fig. S6). The O/W droplets were much more flocculated (than W/O emulsions) and this was reflected by significantly larger $d_{4,3}$ values. Furthermore, the O/W emulsions possessed high viscosities (figure S7a), suggesting that a reinforcing cellulose network was formed in the continuous aqueous phase, as described in the literature [20,24,55,56]. The viscosity flow curves were almost identical for emulsions after 2 weeks storage and the formation of a flocculated network could be confirmed using confocal microscopy (Fig. S7b and c). The CMGs aggregated significantly in the water-continuous phase and formed thick layers between the oil droplets, contributing somewhat to the stabilization against creaming and coalescence. Size distributions, micrographs and images of W/O and O/W emulsions (20 vol% discontinuous phase) with equivalent VH-1 concentrations (0.243 wt% with respect to the continuous phase) are given in Fig. 7. Comparing the two emulsion types, it is evident that much smaller W/O droplets could be

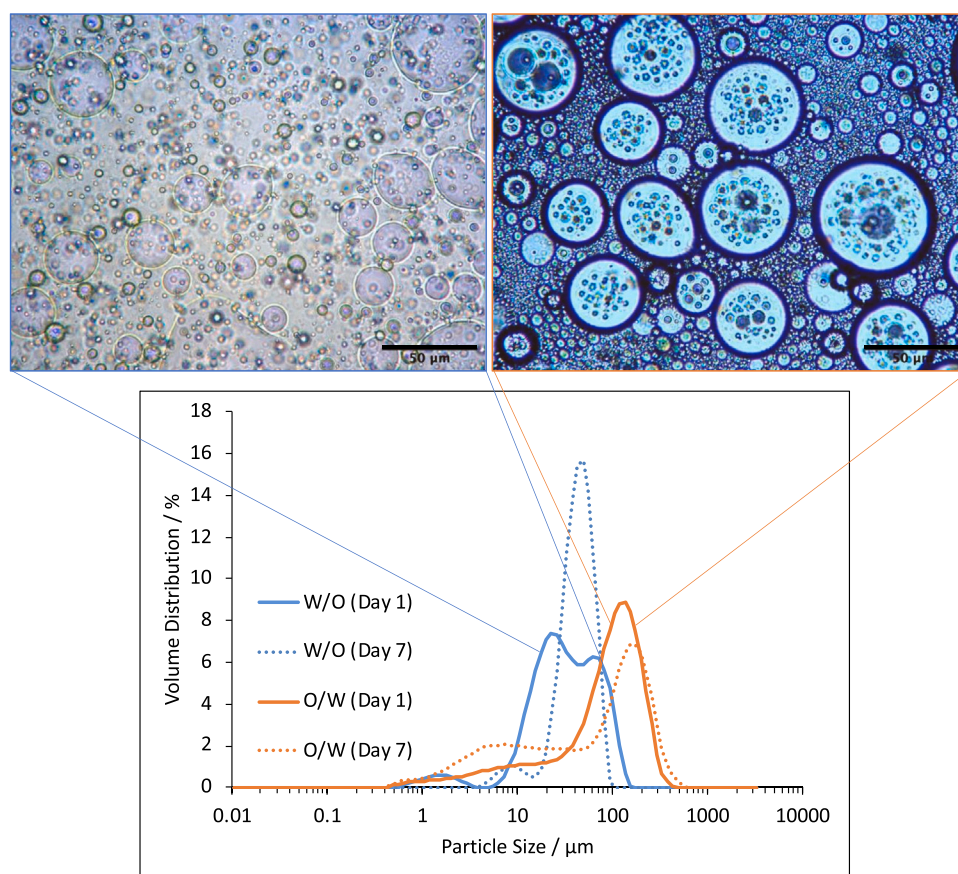


Fig. 7. PSDs of W/O (blue) and O/W (orange) emulsions stabilized by 0.234 wt% VH-1, analyzed over time (day 1 = filled line, day 7 = dashed line); inset gives optical micrographs of freshly prepared W/O (blue border) and O/W (orange border) emulsions. Scale bar = 50 μm , shown at bottom right in black.

produced whilst the O/W oil droplets were much more flocculated. Furthermore, some of the larger CMGs are visible within the large oil droplets for the O/W emulsions, which could in fact be described as a double emulsion (water-in-oil-in-water). Thus the VH-CMGs, as prepared via this alternative 'bottom-up' route, are still more suitable as hydrophobic particulate stabilizers of W/O emulsions, but challenges remain in creating a sufficiently high concentration of these CMGs in the oil phase before emulsification of the water phase.

4.6. Particle size of W/O emulsions stabilized by a combination of H- and VH-CMGs

Out of the three coagulation routes, emulsions stabilized by H-CMGs displayed the best droplet size stability over time. However, the minimum size of droplets that could be achieved was still limited by the size of the CMG particles in the oil phase. Storage instability becomes a greater problem in systems with larger droplets, since droplet coalescence and therefore phase separation can be more likely [57]. Consequently, it was decided to test both H-CMGs and VH-CMGs together, in order to combine the advantages of higher emulsion stability for the former and the creation of smaller, submicron CMGs and droplets for the latter. Confocal micrographs with PSDs overlaid for 20:80 W/O emulsions with H-1 only, VH-1 only and a combination of the two are given below (Fig. 8a, b and c respectively).

From Fig. 8, it appears that the use of H-1 (a) and VH-1 (b) alone leads to a relatively thin coverage of water droplets, compared to when both types of CMG are used together (c). In the absence of VH-CMGs,

only a few, larger droplets were visible after 2 weeks (Fig. S8a) and a large amount of water sedimented out (Fig. S8b). However when a combination of CMGs was used, thicker layers of cellulose were visible at the droplet interface and the average particle size remained stable for at least 14 days (Fig. S8a). More water remained within the emulsion layer (Fig. S8b) and a large number of small droplets were still visible after 2 months (Fig. S8c), indicating enhanced stability.

Using two types of CMG therefore appears to be the best approach to produce stable, W/O emulsions. Whilst the 'medium' sized particles (H-1) allow sufficient concentration of cellulose to be added to the emulsion, the 'smaller' particles (VH-1) diffuse more rapidly to the interface and produce finer dispersions of droplets. Both confocal imaging and cryo-SEM revealed the formation of a thick layer of cellulose (Fig. 9a and b (blue arrow) respectively), with a relatively homogeneous droplet size distribution, explaining the high stability. VH-CMGs displayed a highly regular morphology (Fig. 9b, red arrows) which may allow them to pack more densely at the interface and produce smaller water droplets upon initial emulsification. On the other hand, the larger, heterogeneous H-CMGs require a lower surface coverage and may protrude into the oil phase, providing enhanced steric stability [48]. Therefore, this approach takes advantage of cellulose-cellulose attractive interactions, with effectively two types of uncharged CMGs being introduced.

4.7. Presence of excess CMGs in W/O emulsions stabilized with CMGs

In order to try and gain more information about CMG surface coverage, attempts were made to try and distinguish the 'free,' non-

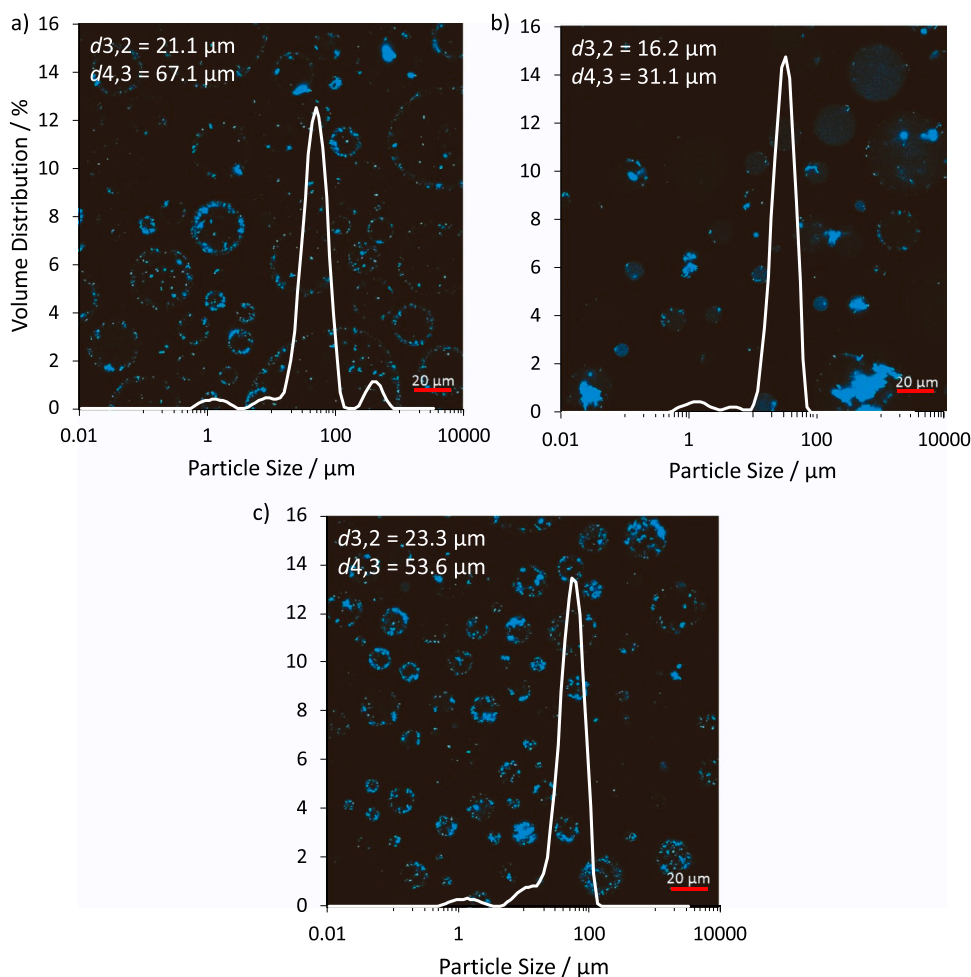


Fig. 8. Confocal micrographs with PSDs overlaid for 20:80 emulsions stabilised by a) H-1 (3 wv.%); b) VH-1 (0.557 wt%) and c) both H-1 and VH-1 (3 wv.% and 0.557 wt%, respectively). Scale bar = 20 μm, shown at bottom right in red, $d_{3,2}$ and $d_{4,3}$ values (μm) are given in the upper left corner.

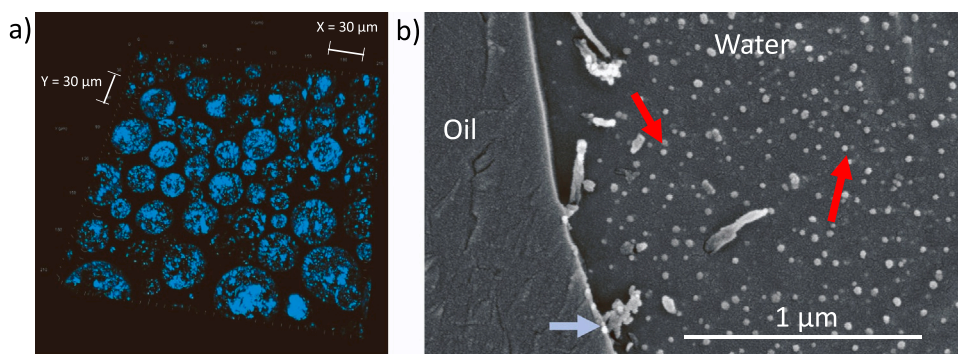


Fig. 9. a) Confocal image of 3D stack of 20:80 W/O emulsion stabilized by H-1 (3 wt%) and VH-1 (0.557 wt%). Scale bar = 30 μm (X and Y axis), depth of 30 μm (Z axis); b) cryo-SEM of 20:80 W/O emulsion stabilized by H-200 (5 wt%) and VH-0.25 (0.267 wt%). Red arrows indicate regular morphology of VH-CMGs; blue arrow indicates thick cellulose layer at the water/oil interface. Scale bar = 1 μm , shown at bottom right in white.

adsorbed CMGs from the CMGs which adsorb to the W/O interface, by generating a PSD for the water droplets alone. Briefly, a set fraction of the CMG-in-oil PSD, (determined from the volume of CMGs dispersed in the oil phase), was subtracted from the W/O volume distribution data (full details can be found in the supporting information, below Fig. S8). In this case we are assuming that the refractive index of the CMGs is roughly the same as water, which should be a valid assumption since the major component of the CMGs is water. Fig. S9 gives an example of PSDs for W/O emulsions stabilized by 2 wt% (a) and 5 wt% (b) L-200, before and after subtraction of the excess CMGs. In general, this subtraction had the effect of marginally reducing the volume distributions at the lower size classes and therefore slightly shifting the average droplet size to higher values. However, the difference between the two was very minor across a range of concentrations and was unable to explain the difference observed between the PSDs and the confocal images.

Some success visualizing the surface coverage in detail was achieved through cryo-SEM. Whilst although evidently not conclusive or quantitative, it confirmed the presence of particles at the droplet interface. In Fig. S10a-c, the droplet surface is clearly rough due to the adsorption of CMGs and a 'coating' of cellulose fibers is visible.

Non-adsorbed CMGs in the continuous oil phase were also difficult to visualize both by CLSM and cryo-SEM, since they were not effectively stained by the Calcofluor White solution and details in the oil phase were difficult to see (respectively). The former may be due to the fact that the dye was introduced in an aqueous medium and/or because the Calcofluor fluorescence is completely quenched in the oil phase. As a result, any excess CMGs in the oil phase are not visible via confocal microscopy,

unlike in the optical images, which therefore appear quite different – it being impossible in the latter to distinguish water droplets from larger CMGs. Brightfield images were overlaid with confocal micrographs in order to visualize the smaller CMGs, since the Calcofluor White signal from the larger CMGs tended to dominate (Fig. S11a). This also allowed visualization of excess CMGs in the oil phase. Furthermore, excitation and emissions experiments of CMG-in-oil and CMG-in-water dispersions both stained by Calcofluor White were conducted, to determine whether different emission filters may be used to selectively detect the CMGs in oil (supporting information, Fig. S11c and d). From these experiments, higher emission wavelengths (i.e. 450–550 nm) were investigated during imaging, and Fig. S11b gives an H-0.25-in-oil dispersion with the adjusted emission filters. This approach was somewhat successful and allowed us to confirm the presence of smaller CMGs in the oil phase, which were completely absent when the standard emission wavelengths were used.

The number-weighted PSDs were also considered and compared to the original volume-weighted PSDs generated by the Mastersizer, since number-average tends to be more influenced by the smaller particles. Fig. 10 gives the confocal micrograph of a 3 wt% CMG-in-oil dispersion (H-0.25) with the brightfield image overlaid, and the corresponding number-weighted and volume-weighted PSDs. As predicted, particle size diameters were much smaller when the number-weighted distributions were considered and a narrower distribution was seen, indicating that probably the majority of the CMG particles in the oil dispersions are within the 1–10 μm range. However, some larger particles and water droplets are present, which fluoresce more strongly and are therefore more visible in the confocal micrographs, causing the

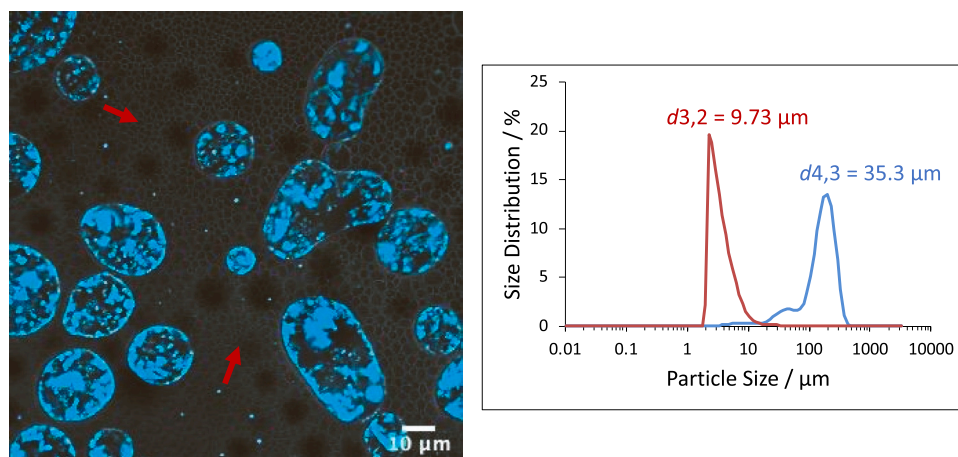


Fig. 10. Confocal micrograph with brightfield image overlaid for a 3 wt% H-0.25 CMG-in-oil dispersion, with the red arrows indicating the individual CMG particles. The number-weighted and volume-weighted PSDs are given on the right in red and blue, respectively. Scale bar = 10 μm , shown at bottom right in white.

volume-weighted PSD to be much higher. We conclude that the volume-weighted PSD is representing the stained, larger water droplets (>ca. 10 μm) and that the number-weighted PSD is representing the smaller, individual CMG particles (<10 μm), visible in the brightfield image. Droplet size analysis conducted using ImageJ agreed with these observations and can be found in the supporting information, (above Fig. S11).

4.8. Rheological analysis of W/O emulsions stabilized by L-AND H-CMGs

To try and gain better understanding of the behavior of excess CMGs in the bulk oil and their possible contribution to emulsion stability, viscosity measurements of the 20:80 W/O emulsions were performed. Since the PSDs of W/O emulsions with various [CMG] appeared to be fairly consistent (Fig. 3b), it was inferred that differences in viscosities should be mainly influenced by changes in the rheological properties of the systems, rather than the droplet size distributions[49].

The flow curves of 20:80 emulsions stabilized by 1–5 wv.% L-200 are given in Fig. 11a. All emulsions initially displayed shear thinning behavior, which may be attributed to some flocculation in the oil phase [58], and a slight increase in viscosity was observed as [CMG] increased (similar to trends in reports for O/W emulsions stabilized by regenerated cellulose [2,59]). This may be due to excess CMGs present in the oil phase at higher concentrations, which would be expected to increase the overall viscosity of the emulsion [60]. Subsequently, a decrease in viscosity of at least 10-fold was observed after 1 day storage for most W/O emulsions (Fig. 11b) and very little further change was observed over 1 week storage (Fig. 11c). At first sight, this observation might be taken as an indication of insufficiently stabilized droplets in the fresh emulsions [61], however confocal micrographs taken over a period of 1 month revealed a relatively stable droplet size, with cellulose still visible at the interface after 30 days and no evidence of bridging flocculation (Fig. 11d). Furthermore, a relatively stable sediment height was recorded, eliminating the possibility of significant water separation

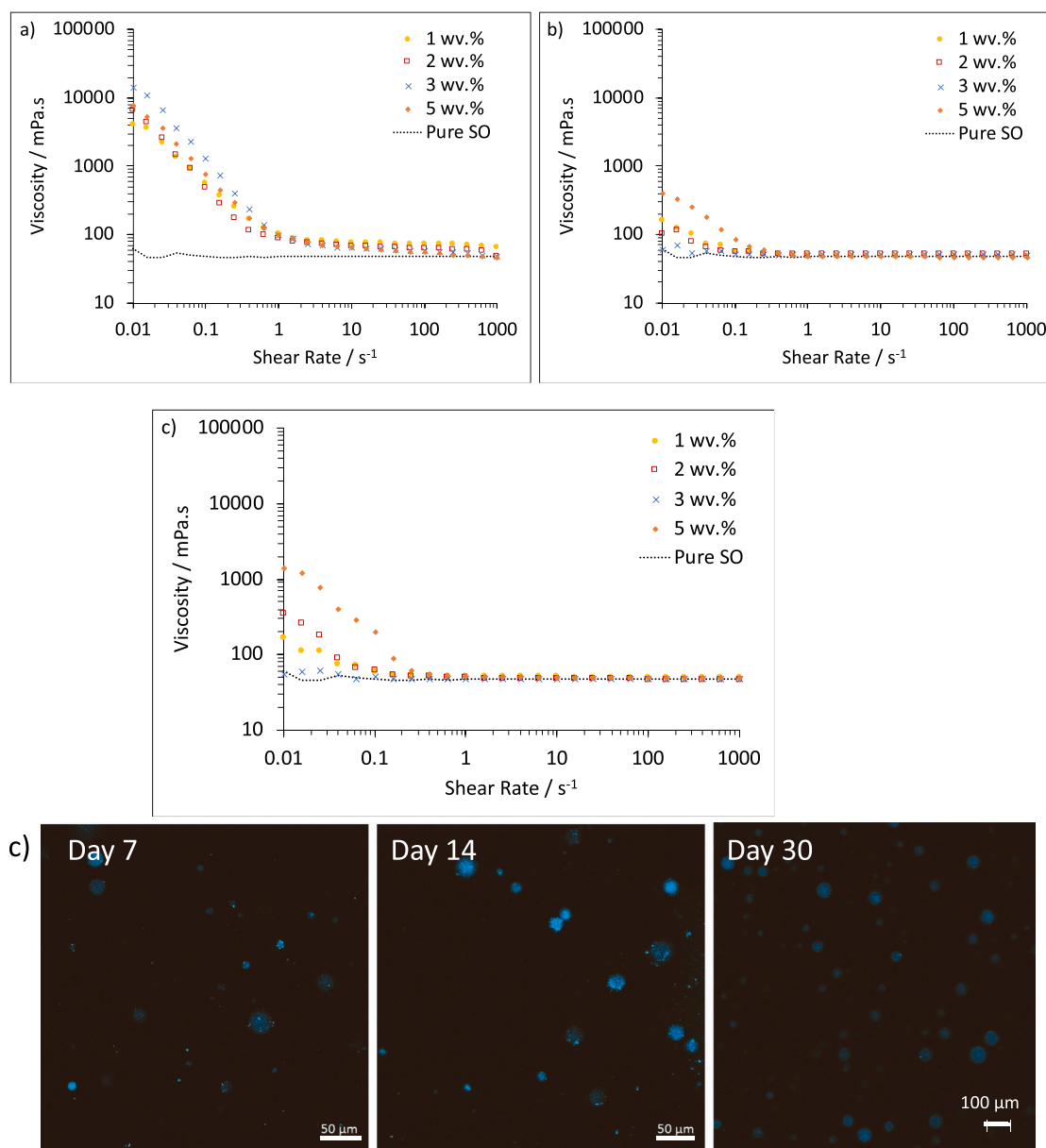


Fig. 11. Flow curves for 20:80 W/O emulsions stabilized by L-200 (1 wv.% = yellow closed circle; 2 wv.% = red open square; 3 wv.% = blue cross and 5 wv.% = orange closed diamond), with pure sunflower oil (dashed black line). Error bars are smaller than the symbols and are therefore not displayed; a) day 1; b) day 2; c) day 7; d) confocal micrographs of 20:80 emulsion stabilized by 5 wv.% CMG-L-200. Scale bars = 50, 50 and 100 μm from left to right, shown at bottom right in white.

occurring.

A reduction in viscosity after 1 day may alternatively be due to adsorption of excess CMGs from the continuous phase to the W/O interface. It has previously been reported that when an excess of microgel particles is present in the continuous phase, microgels at the interface may compress and allow excess microgel to adsorb [62]. This phenomenon occurs when microgels at the interface adopt more flattened structures and spontaneous compression and adsorption of microgels occurs, as opposed to when a densely packed interfacial layer forms initially [63]. Over time, this leads to a more complete droplet coverage and consequently a highly stable emulsion. At [CMG] above the 'threshold' value required for a stable emulsion (>2 wv.%), it is possible that initially excess CMGs are a) dispersing in the continuous phase, or b) forming multilayers at the interface. The former seems more likely, due to the rise in bulk viscosity measured upon increase in [CMG], whilst for the latter, little difference in surface coverage was observed between the 'fresh' emulsions (Fig. 4). However, upon storage an increase in cellulose coverage at the droplet interface was in fact visible using confocal microscopy (Fig. S12). Thick interfacial layers appeared around water droplets whilst little change in droplet size was observed, indicating that excess CMGs may be absorbing from the continuous phase and surface coverage may be increasing. Since the interface initially appears 'unsaturated,' with a small concentration of CMGs sufficient to provide stabilization (2 wv.%), there is sufficient space for excess CMGs to adsorb without the need for significant compression of readily adsorbed microgels (which may be less likely for

stiffer particles, which are expected to undergo smaller deformations) [64] and/or the formation of multilayers. Furthermore, unlike other charged particles more commonly used as Pickering stabilizers [1], the CMGs do not electrostatically repel each other and therefore can pack densely at the interface. Therefore, stability of W/O emulsions appears to be a combination of initially Pickering absorption of smaller CMGs particles, followed by the formation of a thicker interfacial layer with larger CMG particles from the continuous phase, leading to enhanced steric stabilization. This is strikingly different to reports for O/W emulsions, where a cellulose network forms in the water phase over time and leads to a dramatic rise in viscosity, providing an 'indirect' stabilizing effect and delay in droplet coalescence partly due to entrapment [24,55].

4.9. Dilution of W/O emulsions to confirm 'Pickering' mechanism

Finally, W/O emulsions were diluted with oil and analyzed after 6 days storage, in order to confirm the absence of cellulose networks. Fig. 12a gives the flow curves for the original and 10x diluted emulsions, stabilized by H-200 CMGs (5 wv.%) and VH-0.25 (0.237 wt%). The viscosity of the emulsion hardly appeared to change upon dilution, both at this concentration (Fig. 12a) and at a lower concentration (Fig. S13), providing further evidence for a Pickering-type mechanism of stabilization. In addition, the flow curves were almost identical to that of the pure oil (above $\dot{\gamma} = 0.1 \text{ s}^{-1}$) after 1 day storage, indicating the absence of aggregated CMGs in the continuous phase and again supporting the

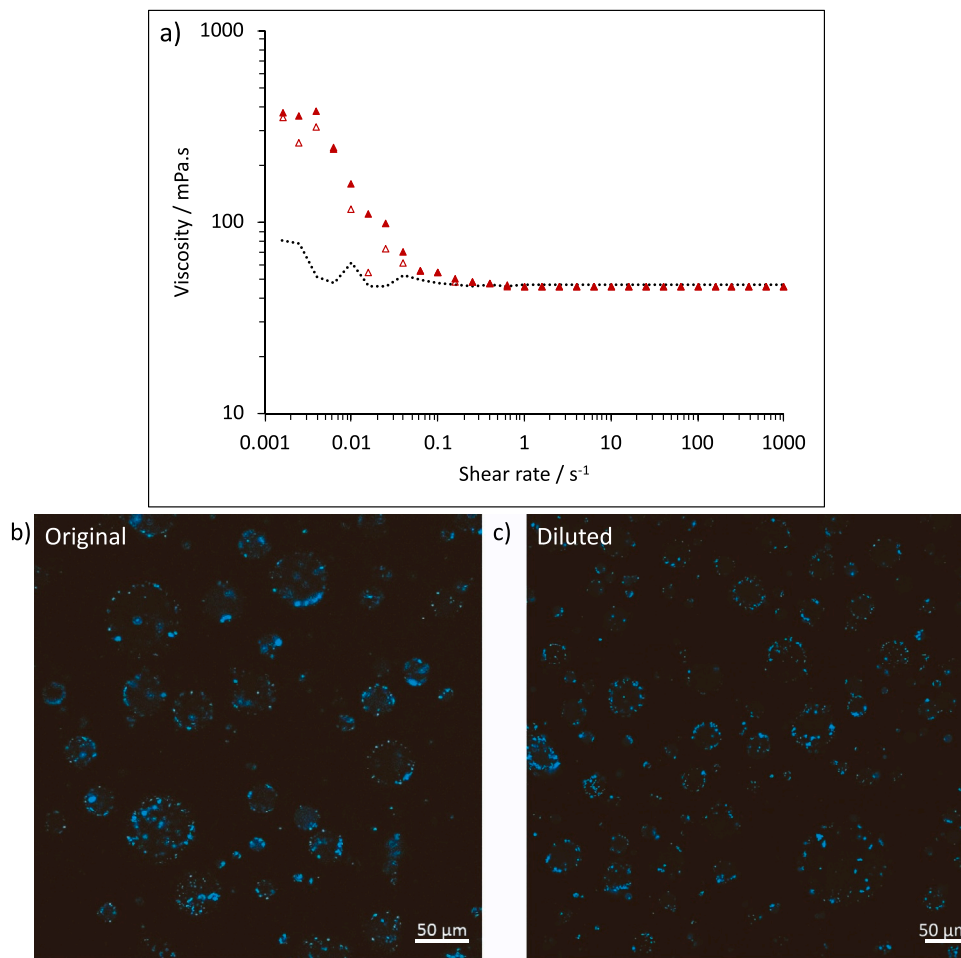


Fig. 12. a) Flow curves for 20:80 W/O emulsions (day 6), stabilized by 5 wv.% H-200 and 0.267 wt% VH-0.25 (closed red triangle = original emulsion; open red triangle = 10x diluted emulsion), with pure sunflower oil (dashed black line). Error bars are all the same size/smaller than the symbols and are therefore not displayed; confocal images of the emulsions on day 6: b) original; c) 10x diluted. Scale bar = 50 μm , shown at bottom right in white.

phenomenon that larger CMGs may absorb over time. This was further evidenced by CLSM (Fig. 12b and c), which clearly revealed CMGs at the interface after 6 days and that coverage did not appear to change upon dilution.

5. Conclusion

In this work, ‘top-down’ and ‘bottom-up’ methods have been used and compared to fabricate ‘hydrophobic’ cellulose stabilizers, via dissolution and coagulation from an IL. It was found that CMG particle size can be reduced by introducing agitation during coagulation, since it is probable that higher shear disrupts the reformation of inter- and intramolecular H-bonds between cellulose chains (to a certain extent). Smaller CMGs could be produced, which dispersed better in the oil-continuous phase and were able to stabilize smaller droplets in the W/O emulsions for a longer period of time. A combination of VH-CMGs (‘small’ particles) and H-CMGs (‘medium’ particles) was found to be the most effective approach, with emulsions displaying high stability for at least 2 months. Confocal microscopy and cryo-SEM revealed thick, interfacial layers in W/O emulsions after storage and viscosity measurements revealed that the stabilization of water is most likely due to interfacial absorption of the CMGs, with no evidence of a cellulose network. Therefore, we propose a mechanism based on a combination of Pickering stabilization followed by subsequent adsorption of excess CMGs to the interface over time. Further investigation into the effect of oil content on the CMG properties and their ability to stabilize oil-continuous systems is currently being carried out. However, this work demonstrates that the properties of CMGs can be optimized for W/O emulsions using physical modification only, and therefore has huge potential for application in the food [65], pharmaceutical [10] and cosmetic [3] industries, among others.

CRedit authorship contribution statement

Katherine S. Lefroy: Conceptualization, Methodology, Data curation, Writing – original draft, Writing – review & editing. **Brent S. Murray:** Conceptualization, Methodology, Supervision, Writing – review & editing. **Michael E. Ries:** Conceptualization, Methodology, Supervision, Writing – review & editing.

Declaration of Competing Interest

The authors declare that they have no known competing financial interests or personal relationships that could have appeared to influence the work reported in this paper.

Acknowledgements

The authors gratefully acknowledge the Engineering and Physical Sciences Research Council (EPSRC) funded Center for Doctoral Training in Soft Matter and Functional Interfaces (SOFI), Grant Ref. no. EP/L015536/1, and Mondelēz International (Reading, UK) for financial support. We would also like to thank Stuart Micklethwaite for carrying out the cryo-SEM analysis and for his help with image analysis. Access to the Zeiss LSM880 inverted microscope was provided by the Bioimaging Facility of the Faculty of Biological Sciences of the University of Leeds.

Appendix A. Supporting information

Supplementary data associated with this article can be found in the online version at [doi:10.1016/j.colsurfa.2022.128926](https://doi.org/10.1016/j.colsurfa.2022.128926).

References

- [1] C. Albert, M. Beladjine, N. Tsapis, E. Fattal, F. Agnely, N. Huang, Pickering emulsions: preparation processes, key parameters governing their properties and

- potential for pharmaceutical applications, *J. Control. Release* 309 (2019) 302–332, <https://doi.org/10.1016/j.jconrel.2019.07.003>.
- [2] D.J. McClements, *Food Emulsions: Principle, Practices, and Techniques*, second ed., CRC Press, Boca Raton, 2004.
- [3] L.L. Schramm, *Personal Care Product Applications*, in: L.L. Schramm (Ed.), *Emuls. Foam. Suspens. Fundam. Appl.*, second ed., Wiley-VCH Verlag GmbH & Co. KGaA, Weinheim, Germany, 2005, pp. 337–346.
- [4] J.B. Cannon, M.A. Long, *Emulsions, microemulsions, and lipid-based drug delivery systems for drug solubilization and delivery—Part II: oral applications*, in: R. Liu (Ed.), *Water-Insoluble Drug Formul.*, second ed., CRC Press, Boca Raton, 2008, pp. 227–254.
- [5] A. Ali, E. Yilmaz, M. Sjöo, A novel technology for personal care emulsions, *Sofwjournal* 141 (2015) 2–7.
- [6] L. Marchetti, B. Muzzio, P. Cerutti, S.C. Andrés, A.N. Califano, Bacterial nanocellulose as novel additive in low-lipid low-sodium meat sausages. Effect on quality and stability, *Food Struct.* 14 (2017) 52–59, <https://doi.org/10.1016/j.foostr.2017.06.004>.
- [7] E. Mitsou, G. Tavantzis, G. Sotiropoulos, D. Ladikos, A. Xenakis, V. Papadimitriou, Food grade water-in-oil microemulsions as replacement of oil phase to help process and stabilization of whipped cream, *Colloids Surf. A Physicochem. Eng. Asp.* 510 (2016) 69–76, <https://doi.org/10.1016/j.colsurfa.2016.07.001>.
- [8] Y. Zhu, X. Luo, X. Wu, W. Li, B. Li, A. Lu, S. Liu, Cellulose gel dispersions: fascinating green particles for the stabilization of oil/water Pickering emulsion, *Cellulose* 24 (2017) 207–217, <https://doi.org/10.1007/s10570-016-1093-9>.
- [9] I. Tavernier, A.R. Patel, P. Van der Meeren, K. Dewettinck, Emulsion-templated liquid oil structuring with soy protein and soy protein: κ-carrageenan complexes, *Food Hydrocoll.* 65 (2017) 107–120, <https://doi.org/10.1016/j.foodhyd.2016.11.008>.
- [10] E. Bouyer, G. Mekhloufi, V. Rosilio, J.L. Grossiord, F. Agnely, Proteins, polysaccharides, and their complexes used as stabilizers for emulsions: alternatives to synthetic surfactants in the pharmaceutical field? *Int. J. Pharm.* 436 (2012) 359–378, <https://doi.org/10.1016/j.ijpharm.2012.06.052>.
- [11] L. Amagliani, C. Schmitt, Globular plant protein aggregates for stabilization of food foams and emulsions, *Trends Food Sci. Technol.* 67 (2017) 248–259, <https://doi.org/10.1016/j.tifs.2017.07.013>.
- [12] A. Sarkar, E. Dickinson, Sustainable food-grade Pickering emulsions stabilized by plant-based particles, *Curr. Opin. Colloid Interface Sci.* 49 (2020) 69–81, <https://doi.org/10.1016/j.cocis.2020.04.004>.
- [13] E. Liwarska-Bizukojc, K. Miksch, A. Malachowska-Jutz, J. Kalka, Acute toxicity and genotoxicity of five selected anionic and nonionic surfactants, *Chemosphere* 58 (2005) 1249–1253, <https://doi.org/10.1016/j.chemosphere.2004.10.031>.
- [14] D. Pimentel, M. Pimentel, Sustainability of meat-based and plant-based diets and the environment, *Am. J. Clin. Nutr.* 78 (2003) 660–663, <https://doi.org/10.1093/ajcn/78.3.660s>.
- [15] B. Pang, H. Liu, P. Liu, X. Peng, K. Zhang, Water-in-oil Pickering emulsions stabilized by stearylated microcrystalline cellulose, *J. Colloid Interface Sci.* 513 (2018) 629–637, <https://doi.org/10.1016/j.jcis.2017.11.079>.
- [16] H. Kang, R. Liu, Y. Huang, Cellulose-based gels, *Macromol. Chem. Phys.* 217 (2016) 1322–1334, <https://doi.org/10.1002/macp.201500493>.
- [17] Y. Habibi, L.A. Lucia, O.J. Rojas, Cellulose nanocrystals: chemistry, self-assembly, and applications, *Chem. Rev.* 110 (2010) 3479–3500, <https://doi.org/10.1021/cr900339w>.
- [18] C. Yamane, T. Aoyagi, M. Ago, K. Sato, K. Okajima, T. Takahashi, Two different surface properties of regenerated cellulose due to structural anisotropy, *Polym. J.* 38 (2006) 819–826, <https://doi.org/10.1295/polymj.PJ2005187>.
- [19] M. Andresen, P. Stenius, Water-in-oil emulsions stabilized by hydrophobized microfibrillated cellulose, *J. Dispers. Sci. Technol.* 28 (2007) 837–844, <https://doi.org/10.1080/01932690701341827>.
- [20] X. Jia, R. Xu, W. Shen, M. Xie, M. Abid, S. Jabbar, P. Wang, X. Zeng, T. Wu, Stabilizing oil-in-water emulsion with amorphous cellulose, *Food Hydrocoll.* 43 (2015) 275–282, <https://doi.org/10.1016/j.foodhyd.2014.05.024>.
- [21] S. Napso, D.M. Rein, Z. Fu, A. Radulescu, Y. Cohen, Structural analysis of cellulose-coated oil-in-water emulsions fabricated from molecular solution, *Langmuir* 34 (2018) 8857–8865, <https://doi.org/10.1021/acs.langmuir.8b01325>.
- [22] T. Winuprasith, M. Suphantharika, Properties and stability of oil-in-water emulsions stabilized by microfibrillated cellulose from mangosteen rind, *Food Hydrocoll.* 43 (2015) 690–699, <https://doi.org/10.1016/j.foodhyd.2014.07.027>.
- [23] S. Napso, D.M. Rein, R. Khalifin, O. Kleinerman, Y. Cohen, Cellulose gel dispersion: from pure hydrogel suspensions to encapsulated oil-in-water emulsions, *Colloids Surf. B Biointerfaces* 137 (2016) 70–76, <https://doi.org/10.1016/j.colsurfb.2015.05.039>.
- [24] Z. Li, H. Wu, M. Yang, D. Xu, J. Chen, H. Feng, Y. Lu, L. Zhang, Y. Yu, W. Kang, Stability mechanism of O/W Pickering emulsions stabilized with regenerated cellulose, *Carbohydr. Polym.* 181 (2018) 224–233, <https://doi.org/10.1016/j.carbpol.2017.10.080>.
- [25] D.M. Rein, R. Khalifin, Y. Cohen, Cellulose as a novel amphiphilic coating for oil-in-water and water-in-oil dispersions, *J. Colloid Interface Sci.* 386 (2012) 456–463, <https://doi.org/10.1016/j.jcis.2012.07.053>.
- [26] R.P. Swatloski, S.K. Spear, J.D. Holbrey, R.D. Rogers, Dissolution of cellulose with ionic liquids, *J. Am. Chem. Soc.* 124 (2002) 4974–4975, <https://doi.org/10.1021/ja025790m>.
- [27] A. Asakawa, T. Oka, C. Sasaki, C. Asada, Y. Nakamura, Cholinium ionic liquid/cosolvent pretreatment for enhancing enzymatic saccharification of sugarcane bagasse, *Ind. Crops Prod.* 86 (2016) 113–119, <https://doi.org/10.1016/j.indcrop.2016.03.046>.

- [28] A. Satlewal, R. Agrawal, S. Bhagia, J. Sangoro, A.J. Ragauskas, Natural deep eutectic solvents for lignocellulosic biomass pretreatment: recent developments, challenges and novel opportunities, *Biotechnol. Adv.* 36 (2018) 2032–2050, <https://doi.org/10.1016/j.biotechadv.2018.08.009>.
- [29] B. Zeng, X. Wang, N. Byrne, Cellulose beads derived from waste textiles for drug delivery, *Polymer* 12 (2020), <https://doi.org/10.3390/polym12071621>.
- [30] E.N. Durmaz, P. Zeynep Culfaz-Emecen, Cellulose-based membranes via phase inversion using [EMIM]OAc-DMSO mixtures as solvent, *Chem. Eng. Sci.* 178 (2018) 93–103, <https://doi.org/10.1016/j.ces.2017.12.020>.
- [31] L. Druel, P. Niemeyer, B. Milow, T. Budtova, Rheology of cellulose-[DBNH][CO2Et] solutions and shaping into aerogel beads, *Green Chem.* 20 (2018) 3993–4002, <https://doi.org/10.1039/c8gc01189c>.
- [32] T. Omura, T. Suzuki, H. Minami, Preparation of cellulose particles with a hollow structure, *Langmuir* 36 (2020) 14076–14082, <https://doi.org/10.1021/acs.langmuir.0c02646>.
- [33] H.J. Kim, J.N. Jin, E. Kan, K.J. Kim, S.H. Lee, Bacterial cellulose-chitosan composite hydrogel beads for enzyme immobilization, *Biotechnol. Bioprocess Eng.* 22 (2017) 89–94, <https://doi.org/10.1007/s12257-016-0381-4>.
- [34] S. Park, S.H. Kim, J.H. Kim, H. Yu, H.J. Kim, Y.H. Yang, H. Kim, Y.H. Kim, S.H. Ha, S.H. Lee, Application of cellulose/lignin hydrogel beads as novel supports for immobilizing lipase, *J. Mol. Catal. B Enzym.* 119 (2015) 33–39, <https://doi.org/10.1016/j.molcatb.2015.05.014>.
- [35] S. Jo, S. Park, Y. Oh, J. Hong, H.J. Kim, K.J. Kim, K.K. Oh, S.H. Lee, Development of cellulose hydrogel microspheres for lipase immobilization, *Biotechnol. Bioprocess Eng.* 24 (2019) 145–154, <https://doi.org/10.1007/s12257-018-0335-0>.
- [36] K.S. Lefroy, B.S. Murray, M.E. Ries, T.D. Curwen, A natural, cellulose-based microgel for water-in-oil emulsions, *Food Hydrocoll.* 113 (2021), 106408, <https://doi.org/10.1016/j.foodhyd.2020.106408>.
- [37] R.M. Wiley, Limited coalescence of oil droplets in coarse oil-in-water emulsions, *J. Colloid Sci.* 9 (1954) 427–437, [https://doi.org/10.1016/0095-8522\(54\)90030-6](https://doi.org/10.1016/0095-8522(54)90030-6).
- [38] K.S. Lefroy, B.S. Murray, M.E. Ries, Advances in the use of microgels as emulsion stabilisers and as a strategy for cellulose functionalisation, *Cellulose* 28 (2021) 647–670, <https://doi.org/10.1007/s10570-020-03595-8>.
- [39] Z. Fan, J. Chen, W. Guo, F. Ma, S. Sun, Q. Zhou, Crystallinity of regenerated cellulose from [Bmim]Cl dependent on the hydrogen bond acidity/basicity of anti-solvents, *RSC Adv.* 7 (2017) 41004–41010, <https://doi.org/10.1039/c7ra08178b>.
- [40] Z. Fan, J. Chen, W. Guo, F. Ma, S. Sun, Q. Zhou, Anti-solvents tuning cellulose nanoparticles through two competitive regeneration routes, *Cellulose* 25 (2018) 4513–4523, <https://doi.org/10.1007/s10570-018-1897-x>.
- [41] K.S. Lefroy, B.S. Murray, M.E. Ries, Rheological and NMR Studies of Cellulose Dissolution in the Ionic Liquid BmimAc, *J. Phys. Chem. B* 125 (2021) 8205–8218, <https://doi.org/10.1021/acs.jpcc.1c02848>.
- [42] I. Burgaud, E. Dickinson, P.V. Nelson, An improved high-pressure homogenizer for making fine emulsions on a small scale, *Int. J. Food Sci. Technol.* 25 (1990) 39–46, <https://doi.org/10.1111/j.1365-2621.1990.tb01057.x>.
- [43] L. Pravinata, M. Akhtar, P.J. Bentley, T. Mahatnirunkul, B.S. Murray, Preparation of alginate microgels in a simple one step process via the Leeds Jet Homogenizer, *Food Hydrocoll.* 61 (2016) 77–84, <https://doi.org/10.1016/j.foodhyd.2016.04.025>.
- [44] M.R. Islam, L.A. Lyon, Deswelling studies of pH and temperature-sensitive ultra-low cross-linked microgels with cross-linked cores, *Colloid Polym. Sci.* 298 (2020) 395–405, <https://doi.org/10.1007/s00396-020-04620-9>.
- [45] E. Dickinson, Hydrocolloids as emulsifiers and emulsion stabilizers, *Food Hydrocoll.* 23 (2009) 1473–1482, <https://doi.org/10.1016/j.foodhyd.2008.08.005>.
- [46] E. Dickinson, The structure and stability of emulsions, in: J.M.V. Blanshard, J. R. Mitchell (Eds.), *Food Struct. - Its Creat. Eval.*, Woodhead Publishing, Cambridge, 1988, pp. 41–57.
- [47] H. Dai, J. Wu, H. Zhang, Y. Chen, L. Ma, H. Huang, Y. Huang, Y. Zhang, Recent advances on cellulose nanocrystals for Pickering emulsions: development and challenge, *Trends Food Sci. Technol.* 102 (2020) 16–29, <https://doi.org/10.1016/j.tifs.2020.05.016>.
- [48] I. Capron, O.J. Rojas, R. Bordes, Behavior of nanocelluloses at interfaces, *Curr. Opin. Colloid Interface Sci.* 29 (2017) 83–95, <https://doi.org/10.1016/j.cocis.2017.04.001>.
- [49] B. Medronho, A. Filipe, C. Costa, A. Romano, B. Lindman, H. Edlund, M. Norgren, Micro-rheology of novel cellulose stabilized oil-in-water emulsions, *J. Colloid Interface Sci.* 531 (2018) 225–232, <https://doi.org/10.1016/j.jcis.2018.07.043>.
- [50] C. Costa, B. Medronho, B. Lindman, H. Edlund, M. Norgren, Cellulose as a natural emulsifier: from nanocelluloses to macromolecules, *Cellul. Sci. Deriv.* (2021), <https://doi.org/10.5772/intechopen.99139>.
- [51] A. Hedlund, H. Theliander, T. Köhnke, Mass transport during coagulation of cellulose-ionic liquid solutions in different non-solvents, *Cellulose* 26 (2019) 8525–8541, <https://doi.org/10.1007/s10570-019-02649-w>.
- [52] H.P. Fink, P. Weigel, H.J. Purz, J. Ganster, Structure formation of regenerated cellulose materials from NMMO-solutions, *Prog. Polym. Sci.* 26 (2001) 1473–1524, [https://doi.org/10.1016/S0079-6700\(01\)00025-9](https://doi.org/10.1016/S0079-6700(01)00025-9).
- [53] S.O. Ilyin, V.V. Makarova, T.S. Anokhina, V.Y. Ignatenko, T.V. Brantseva, A. V. Volkov, S.V. Antonov, Diffusion and phase separation at the morphology formation of cellulose membranes by regeneration from N-methylmorpholine N-oxide solutions, *Cellulose* 25 (2018) 2515–2530, <https://doi.org/10.1007/s10570-018-1756-9>.
- [54] A. Hedlund, T. Köhnke, J. Hagman, U. Olsson, H. Theliander, Microstructures of cellulose coagulated in water and alcohols from 1-ethyl-3-methylimidazolium acetate: contrasting coagulation mechanisms, *Cellulose* 26 (2019) 1545–1563, <https://doi.org/10.1007/s10570-018-2168-6>.
- [55] K.P. Oza, S.G. Frank, Microcrystalline cellulose stabilized emulsions, *J. Dispers. Sci. Technol.* 7 (1986) 543–561, <https://doi.org/10.1080/01932698608943478>.
- [56] Y. Ni, J. Li, L. Fan, Production of nanocellulose with different length from ginkgo seed shells and applications for oil in water Pickering emulsions, *Int. J. Biol. Macromol.* 149 (2020) 617–626, <https://doi.org/10.1016/j.ijbiomac.2020.01.263>.
- [57] L. Bai, S. Huan, W. Xiang, O.J. Rojas, Pickering emulsions by combining cellulose nanofibrils and nanocrystals: phase behavior and depletion stabilization, *Green Chem.* 20 (2018) 1571–1582, <https://doi.org/10.1039/c8gc00134k>.
- [58] M. Zembyla, A. Lazidis, B.S. Murray, A. Sarkar, Stability of water-in-oil emulsions co-stabilized by polyphenol crystal-protein complexes as a function of shear rate and temperature, *J. Food Eng.* 281 (2020), 109991, <https://doi.org/10.1016/j.jfoodeng.2020.109991>.
- [59] W. Shen, L. Guo, T. Wu, W. Zhang, M. Abid, Stabilizing beverage emulsions by regenerated celluloses, *LWT - Food Sci. Technol.* 72 (2016) 292–301, <https://doi.org/10.1016/j.lwt.2016.05.012>.
- [60] C. Costa, P. Rosa, A. Filipe, B. Medronho, A. Romano, L. Liberman, Y. Talmon, M. Norgren, Cellulose-stabilized oil-in-water emulsions: structural features, micro-rheology, and stability, *Carbohydr. Polym.* 252 (2021), 117092, <https://doi.org/10.1016/j.carbpol.2020.117092>.
- [61] B. Brugger, B.A. Rosen, W. Richtering, Microgels as stimuli-responsive stabilizers for emulsions, *Langmuir* 24 (2008) 12202–12208, <https://doi.org/10.1021/la8015854>.
- [62] F. Pinaud, K. Geisel, P. Massé, B. Catargi, L. Isa, W. Richtering, V. Ravaine, V. Schmitt, Adsorption of microgels at an oil-water interface: correlation between packing and 2D elasticity, *Soft Matter* 10 (2014) 6963–6974, <https://doi.org/10.1039/c4sm00562g>.
- [63] V. Schmitt, V. Ravaine, Surface compaction versus stretching in Pickering emulsions stabilised by microgels, *Curr. Opin. Colloid Interface Sci.* 18 (2013) 532–541, <https://doi.org/10.1016/j.cocis.2013.11.004>.
- [64] K. Geisel, L. Isa, W. Richtering, Unraveling the 3D localization and deformation of responsive microgels at oil/water interfaces: a step forward in understanding soft emulsion stabilizers, *Langmuir* 28 (2012) 15770–15776, <https://doi.org/10.1021/la302974j>.
- [65] B. Ozturk, D.J. McClements, Progress in natural emulsifiers for utilization in food emulsions, *Curr. Opin. Food Sci.* 7 (2016) 1–6, <https://doi.org/10.1016/j.cofs.2015.07.008>.